Synthesis of Tantalum(V) Amido Silyl Complexes and the Unexpected Formation of $(Me_2N)_3Ta(\eta^2\text{-}ONMe_2)[OSi(SiMe_3)_3]$ from the Reaction of $(Me_2N)_4Ta[Si(SiMe_3)_3]$ with O_2

Zhongzhi Wu, Hu Cai, Xianghua Yu, Jaime R. Blanton, Jonathan B. Diminnie, Hong-Jun Pan, and Ziling Xue*

Department of Chemistry, The University of Tennessee, Knoxville, Tennessee 37996-1600

Jeffrey C. Bryan

Chemical Sciences Division, Oak Ridge National Laboratory, Oak Ridge, Tennessee 37831-6181

Received July 9, 2002

The synthesis and characterization of amido silyl complexes of tantalum(V) free of π-anionic ligands are reported. The amido silyl chloride complexes $(Me_2N)_3Ta(SiR_3)Cl$ [SiR_3 = $Si(SiMe_3)_3$ (**1a**), $SiPh_2Bu^t$ (**2**)] were prepared from $(Me_2N)_3TaCl_2$ and the corresponding silyllithium reagents $Li(THF)_3Si(SiMe_3)_3$ and $Li(THF)_3SiPh_2Bu^t$. The amido silyl complexes $(Me_2N)_4Ta(SiR_3)$ [SiR_3 = $Si(SiMe_3)_3$ (**3**), $SiPh_2Bu^t$ (**4**)] were synthesized by the reactions of $(Me_2N)_4TaCl$ with $Li(THF)_3SiR_3$. Complex **3** was found to react with 1 equiv of O_2 to give an oxidation product $(Me_2N)_3Ta(\eta^2\text{-}ONMe_2)[OSi(SiMe_3)_3]$ (**5**), and the structure of **5** was confirmed by X-ray crystallography. The spectroscopic data and crystal structure determination reveal that the coordination geometry around Ta metal in **1a** and **2**−**4** is trigonal bipyramid with silyl ligands in an equatorial position.

Early-transition-metal amido complexes have attracted much attention in recent years in part because of their important applications as precursors in chemical vapor deposition of microelectronic metal nitride (MN_x) and M−Si−N ternary films as diffusion barriers in Si-based microelectronic devices.[1,2] In particular, M−Si−N ternary films, which are often amorphous, have shown better diffusion barrier properties than, e.g., TiN films that are usually polycrystalline and thus have grain boundaries for diffusion.[1c,d,2] Although numerous well-characterized Ta amido complexes[3] and several Ta silyl complexes[4] have been reported, few Ta(V) amido silyl complexes are known.[4i,5] Cp-free early-transition-metal amido silyl complexes are of interest in part as they are potential precursors to Ta−Si−N ternary materials. We report herein preparation and structural characterization of a series of Ta(V) amido silyl complexes $(Me_2N)_3Ta(SiR_3)Cl$ [SiR_3 = $Si(SiMe_3)_3$ (**1**),[6] $SiPh_2Bu^t$ (**2**)] and $(Me_2N)_4Ta(SiR_3)$ [SiR_3 = $Si(SiMe_3)_3$ (**3**), $SiPh_2Bu^t$ (**4**)], as well as an oxidation product $(Me_2N)_3Ta(\eta^2\text{-}ONMe_2)[OSi(SiMe_3)_3]$ (**5**).

Experimental Section

General Procedures. All manipulations were performed under a dry nitrogen atmosphere with the use of either standard Schlenk techniques or a glovebox. Solvents were purified by distillation over potassium/benzophenone ketyl. Benzene-d_6 and toluene-d_8 were dried over activated molecular sieves and stored under nitrogen. $TaCl_5$ (Strem) was sublimed prior to use. $LiNMe_2$ (Aldrich) was used as received. $(Me_2N)_3TaCl_2$,[7] $(Me_2N)_4TaCl$,[8] and $Li(THF)_3SiBu^tPh_2$[9a] were prepared

(1) (a) Musher, J. N.; Gordon, R. G. *J. Electrochem. Soc.* **1996**, *143*, 736. (b) Hoffman, D. M. *Polyhedron* **1994**, *13*, 1169. (c) Winter, C. H. *Aldrichim. Acta* **2000**, *33*, 3. (d) Kaloyeros, A. E.; Eisenbraun, E. *Annu. Rev. Mater. Sci.* **2000**, *30*, 363.

(2) Custer, J. S.; Smith, P. M.; Fleming, J. G.; Roherty-Osmum, E. *Am. Chem. Soc. Symp. Ser.* **1999**, *727*, 86.

(3) (a) Lappert, M. F.; Power, P. P.; Sanger, A. R.; Srivastava, R. C. *Metal and Metalloid Amides*; Ellis Horwood: New York, 1980. (b) Chisholm, M. H.; Rothwell, I. P. In *Comprehensive Coordination Chemistry*; Wilkinson, G., Gillard, R. D., McCleverty, J. A., Eds.; Pergamon: New York, 1987; Vol. 2.

(4) (a) Curtis, M. D.; Bell, L. G.; Butler, W. M. *Organometallics* **1985**, *4*, 701. (b) Arnold, J.; Shina, D. N.; Tilley, T. D.; Arif, A. M. *Organometallics* **1986**, *5*, 2037. (c) Jiang, Q.; Carroll, P. J.; Berry, D. H. *Organometallics* **1991**, *10*, 3648. (d) Xue, Z.-L.; Li, L.-T.; Hoyt, L. K.; Diminnie, J. B.; Pollitte, J. L. *J. Am. Chem. Soc.* **1994**, *116*, 2169. (e) Li, L.; Diminnie, J. B.; Liu, X.; Pollitte, J. L.; Xue, Z.-L. *Organometallics* **1996**, *15*, 3520. (f) Liu, X.; Li, L.; Diminnie, J. B.; Yap, G. P. A.; Rheingold, A. L.; Xue, Z.-L. *Organometallics* **1998**, *17*, 4597. (g) Burckhardt, U.; Casty, G. L.; Tilley, T. D.; Woo, T. K.; Rothlisberger, U. *Organometallics* **2000**, *19*, 3830. (h) Nikonov, G. I.; Mountford P.; Green, J. C.; Cooke, P. A.; Leech, M. A.; Blake, A. J.; Howard, J. A. K.; Lemenovskii, D. A. *Eur. J. Inorg. Chem.* **2000**, 1917. (i) Wu, Z.-Z.; Xue, Z.-L. *Organometallics* **2000**, *19*, 4191. (j) Diminnie, J. B.; Hall, H. D.; Xue, Z.-L. *J. Chem. Soc., Chem. Commun.* **1996**, 2383.

(5) (a) Tilley, T. D. In *The Chemistry of Organic Silicon Compounds*; Patai, S., Rappoport, Z., Eds.; Wiley: New York, 1989; Chapter 24. (b) Tilley, T. D. In *The Silicon-Heteroatom Bond*; Patai, S., Rappoport, Z., Eds.; Wiley: New York, 1991; Chapters 9 and 10. (c) Eisen, M. S. In *The Chemistry of Organic Silicon Compounds*; Rappoport, Z., Apeloig, Y., Eds.; Wiley: New York, 1998; Vol. 2, Part 3, p 2037. (d) Tilley, T. D. *Comments Inorg. Chem.* **1990**, *10*, 37. (e) Harrod, J. F.; Mu, Y.; Samuel, E. *Polyhedron* **1991**, *10*, 1239. (f) Corey, J. Y. In *Advances in Silicon Chemistry*; Larson, G., Ed.; JAI Press: Greenwich, CT, 1991; Vol. 1, p 327. (g) Tilley, T. D. *Acc. Chem. Res.* **1993**, *26*, 22. (h) Sharma, H. K.; Pannell, K. H. *Chem. Rev.* **1995**, *95*, 1351. (i) Xue, Z. *Comments Inorg. Chem.* **1996**, *18*, 223. (j) Chen, T.; Xue, Z. *Chinese J. Inorg. Chem.* **1999**, *15*, 413.

(6) Preliminary results of the synthesis of **1** have been reported: Wu, Z.-Z.; Diminnie, J. B.; Xue, Z.-L. *J. Am. Chem. Soc.* **1999**, *121*, 4300.

10.1021/om020537g CCC: $22.00
Publication on Web 08/21/2002

according to literature procedures. $Li(THF)_3Si(SiMe_3)_3$ was prepared from $Si(SiMe_3)_4$ and MeLi/LiBr and crystallized before use.[9b] ^1H and ^{13}C NMR spectra were recorded on a Bruker AC-250 or AMX 400 Fourier transform spectrometer and referenced to the solvents (residue protons in the ^1H NMR spectra). ^{29}Si NMR data were obtained on an AMX 400 Fourier transform spectrometer and referenced to $SiMe_4$. ^1H EXSY (Exchange Spectroscopy) spectroscopy was conducted on a Varian INOVA 600 high-resolution NMR spectrometer. Elemental analyses were performed by E+R Microanalytical Laboratory (Parsippany, New Jersey).

Preparation of $(Me_2N)_3Ta[Si(SiMe_3)_3]Cl$ (1a). To a yellow slurry of $(Me_2N)_3TaCl_2$ (0.50 g, 1.30 mmol) in hexanes (20 mL) was added dropwise 1 equiv of $Li(THF)_3Si(SiMe_3)_3$ (0.65 g, 1.40 mmol) in hexanes (20 mL) with stirring. The solution was stirred at room temperature for 3 h. The removal of volatiles afforded a yellow solid, which was identified to be **1a**. NMR of **1a**: ^1H NMR (benzene-d_6, 250.1 MHz, 23 °C) δ 3.10 (s, 12H, N*Me*$_2$), 0.50 (s, 27H, Si*Me*$_3$); (toluene-d_8, 400.2 MHz, 23 °C) δ 3.14 (s, 12H, N*Me*$_2$), 0.47 (s, 27H, Si*Me*$_3$); ^1H NMR (THF-d_8, 400.2 MHz, 23 °C) δ 3.48 (s, 12H, N*Me*$_2$), 0.29 (s, 27H, Si*Me*$_3$). $^{13}C\{^1H\}$ NMR (benzene-d_6, 62.9 MHz, 23 °C) δ 43.45 (N*Me*$_2$), 5.77 (Si*Me*$_3$). $^{29}Si\{^1H\}$ NMR (DEPT, toluene-d_8, 79.5 MHz, −40 °C) δ 4.24 (Si*Si*Me$_3$), −51.34 (*Si*SiMe$_3$). Extraction of the solid with pentane, followed by filtration and crystallization at −20 °C yielded yellow crystals (0.38 g). During the crystallization process, **1a** was found to react with LiBr, which was present in $Li(THF)_3Si(SiMe_3)_3$, to give $(Me_2N)_3Ta[Si(SiMe_3)_3]Br$ (**1b**), a bromide analogue of **1a**, as a crystalline mixture with **1a**. NMR of **1b**: ^1H NMR (benzene-d_6, 250.1 MHz, 23 °C) δ 3.07 (s, 12H, N*Me*$_2$), 0.49−0.50 (s, 27H, Si*Me*$_3$); ^1H NMR (toluene-d_8, 400.2 MHz, 23 °C) δ 3.10 (s, 12H, N*Me*$_2$), 0.46−0.47 (s, 27H, Si*Me*$_3$); ^1H NMR (THF-d_8, 400.2 MHz, 23 °C) 3.46 (s, 12H, N*Me*$_2$) and 0.30 (s, 27H, Si*Me*$_3$). $^{13}C\{^1H\}$ NMR (benzene-d_6, 62.9 MHz, 23 °C) δ 43.45 (N*Me*$_2$), 5.86 (Si*Me*$_3$). $^{29}Si\{^1H\}$ NMR (DEPT, toluene-d_8, 79.5 MHz, −40 °C) δ 4.39 (Si*Si*Me$_3$), −51.34 (*Si*SiMe$_3$). The NMR of the yellow crystals (0.38 g) revealed that they were a 3:2 molar mixture of **1a** and **1b** (formula $C_{15}H_{45}Br_{0.4}Cl_{0.6}N_3Si_4Ta$; fw 610.99; 0.62 mmol, 48% yield). Anal. Calcd for $C_{15}H_{45}ClN_3Si_4Ta$ (**1a**): C, 30.21; H, 7.61. For a 3:2 molar mixture of **1a** and **1b**: C, 29.33; H, 7.39. Found for a 3:2 mixture of **1a** and **1b**: C, 30.05; H, 7.39.

Addition of LiBr and THF to a toluene-d_8 solution of **1a** and **1b** was found to increase the intensity of the peaks of **1b** in the ^1H NMR spectra of the solution, and reduce those of **1a**, thus confirming the identification of this bromide analogue of **1a**.

Preparation of $(Me_2N)_3Ta(SiPh_2Bu^t)Cl$ (2). A slurry of $(Me_2N)_3TaCl_2$ (1.00 g, 2.60 mmol) in toluene (20 mL) was treated with 1 equiv of $Li(THF)_3SiPh_2Bu^t$ (1.21 g, 2.62 mmol) in toluene (20 mL) at −20 °C. After the mixture was stirred for 4 h at room temperature, the volatiles were removed in vacuo. The yellow solid was extracted with pentane, and the solution was filtered, concentrated, and cooled to −20 °C to afford 0.46 g (0.78 mmol, 30% yield) of yellow crystals of **2**. ^1H NMR (benzene-d_6, 250.1 MHz, 23 °C) δ 7.97−7.14 (m, 10H, C_6H_5), 2.87 (s, 18H, N*Me*$_2$), 1.50 (s, 9H, C*Me*$_3$). ^{13}C NMR (benzene-d_6, 62.9 MHz, 23 °C) δ 144.9, 137.6, 127.8, 127.7 (C_6H_5), 42.8 (N*Me*$_2$), 30.5 (C*Me*$_3$), 25.2 (*C*Me$_3$). $^{29}Si\{^1H\}$ NMR (DEPT, benzene-d_6, 79.5 MHz, 23 °C) δ 64.6 (*Si*Ph$_2$Bu^t). Anal. Calcd for $C_{22}H_{37}ClN_3SiTa$: C, 44.94; H, 6.34. Found: C, 44.85; H, 6.35.

Preparation of $(Me_2N)_4TaSi(SiMe_3)_3$ (3). A yellow solution of $(Me_2N)_4TaCl$ (1.00 g, 2.55 mmol) in hexanes (20 mL) was treated with 1 equiv of $Li(THF)_3Si(SiMe_3)_3$ (1.27 g, 2.70 mmol) in hexanes (20 mL) at room temperature. The reaction mixture was stirred for 3 h, and the NMR spectrum shows that the formation of **3** is almost quantitative. The solvent was then removed in vacuo, and the yellow residue was extracted with pentane. The solution was filtered, concentrated, and cooled to −20 °C to afford red-orange crystals of **3** (0.45 g, 0.75 mmol, 30% yield). Repeated attempts to obtain pure **3** were unsuccessful, and the structural assignment for **3** was thus made based on the analysis of its spectroscopic data and its reaction with O_2 to form **5**, which is discussed below. ^1H NMR (benzene-d_6, 250.1 MHz, 23 °C) δ 3.13 (s, 24H, N*Me*$_2$), 0.45 (s, 27H, Si*Me*$_3$). ^{13}C NMR (benzene-d_6, 62.9 MHz, 23 °C) δ 45.4 (N*Me*$_2$), 6.4 (Si*Me*$_3$). $^{29}Si\{^1H\}$ NMR (DEPT, benzene-d_6, 79.5 MHz, 23 °C) δ −4.0 (Si*Si*Me$_3$), −98.4 (*Si*SiMe$_3$).

Preparation of $(Me_2N)_4TaSiPh_2Bu^t$ (4). A solution of $Li(THF)_3SiPh_2Bu^t$ (1.27 g, 2.75 mmol) in Et_2O (20 mL) was added dropwise with stirring to a solution of $(Me_2N)_4TaCl$ (1.08 g, 2.75 mmol) in Et_2O (20 mL) at −20 °C. After the mixture was stirred at room temperature for 2 h, the volatiles were removed in vacuo. The yellow-orange residue was extracted with hexanes, and the solution was filtered, concentrated, and cooled to −20 °C to yield 0.51 g (0.85 mmol, 31% yield) of yellow-orange crystals of **4**. ^1H NMR (benzene-d_6, 250.1 MHz, 23 °C) δ 7.82−7.15 (m, 10H, C_6H_5), 3.11 (s, 24H, N*Me*$_2$), 1.43 (s, 9H, C*Me*$_3$). ^{13}C NMR (benzene-d_6, 62.9 MHz, 23 °C) δ 147.8, 137.2, 127.3, 127.1 (C_6H_5), 46.1 (N*Me*$_2$), 31.9 (C*Me*$_3$), 25.3 (*C*Me$_3$). $^{29}Si\{^1H\}$ NMR (DEPT, benzene-d_6, 79.5 MHz, 23 °C) δ −189.0 (*Si*Ph$_2$Bu^t). Anal. Calcd for $C_{24}H_{43}N_4SiTa$: C, 48.31; H, 7.26. Found: C, 48.41; H, 7.24.

Preparation of $(Me_2N)_3Ta(\eta^2\text{-}ONMe_2)[OSi(SiMe_3)_3]$ (5). To a benzene solution of **3** (1.50 g, 2.48 mmol) was introduced 1 equiv of dry O_2. The red-orange solution of **3** gradually turned yellow-orange at room temperature. After the solution was stirred overnight at room temperature, NMR spectra showed that ca. 80% of **3** had been converted to **5**. Removal of the volatiles in vacuo, followed by extraction with pentane and crystallization at −20 °C afforded yellow crystals of **5** (0.45 g, 0.71 mmol, 28% yield). ^1H NMR (benzene-d_6, 250.1 MHz, 23 °C) δ 3.30 (s, 18H, Ta−N*Me*$_2$), 2.49 (s, 6H, ON*Me*$_2$), 0.33 (s, 27H, Si*Me*$_3$). ^{13}C NMR (benzene-d_6, 62.9 MHz, 23 °C) δ 49.6 (ON*Me*$_2$), 47.1 (Ta−N*Me*$_2$), 1.0 (Si*Me*$_3$). $^{29}Si\{^1H\}$ NMR (DEPT, benzene-d_6, 79.5 MHz, 23 °C) δ −13.7 (Si*Si*Me$_3$), −16.8 (*Si*SiMe$_3$). Anal. Calcd for $C_{17}H_{51}N_4O_2Si_4Ta$: C, 32.06; H, 8.07. Found: C, 31.87; H, 7.88.

X-ray Crystal Structure Determination of 1a/1b, 2, 4, and 5. Crystal data and a summary of intensity data collection parameters for **1a**/**1b**, **2**, **4**, and **5** are given in Table 1.

Two crystal structures of **1a**/**1b** were determined. **1a** and **1b** were found to co-crystallize in crystals, and repeated attempts to obtain the structure of **1a** or **1b** were unsuccessful.

The first structure of **1a**/**1b** was determined on a Siemens R3m/V diffractometer equipped with a graphite-monochromated Mo source ($K\alpha$ radiation, 0.71073 Å) and fitted with a Nicolet LT-2 low-temperature device. Suitable crystals were coated with Paratone oil (Exxon) and mounted under a stream of N_2 at −100 °C. The unit cell parameters [a = 15.425(5) Å, b = 9.814(4) Å, c = 18.337(7) Å, α = 90°, β = 91.96(3)°, γ = 90°] and orientation matrix were determined from a least-squares fit of the orientation of at least 35 reflections obtained from a rotation photo and an automatic peak search routine. The structures were solved by direct methods. Non-hydrogen atoms were anisotropically refined except for the disordered Cl (Br) atom. The largest electron density in the final difference map of **1a** is ca. 0.5 Å away from the Cl atom. All hydrogen atoms were placed in calculated positions and introduced into the refinement as fixed contributors with an isotropic U value of 0.08 Å^2. All calculations were performed with use of the Siemens SHELXTL 93 (version 5.0) software package. An ORTEP view of the structure and the report of the crystal structure are given in the Supporting Information.

(7) Chisholm, M. H.; Huffman, J. C.; Tan, L.-S. *Inorg. Chem.* **1981**, *20*, 1859.
(8) Chisholm, M. H.; Tan, L.-S.; Huffman, J. C. *J. Am. Chem. Soc.* **1982**, *104*, 4879.
(9) (a) Campion, B. K.; Heyn, R. H.; Tilley, T. D. *Organometallics* **1993**, *12*, 2584. (b) Gutekunst, G.; Brook, A. G. *J. Organomet. Chem.* **1982**, *225*, 1.

Table 1. Crystallographic Data for 1a/1b, 2, 4, and 5

	1a/1b	2	4	5
formula	$C_{15}H_{45}Br_{0.281}Cl_{0.719}N_3Si_4Ta$	$C_{22}H_{37}ClN_3SiTa$	$C_{24}H_{43}ClN_4SiTa$	$C_{17}H_{51}N_4O_2Si_4Ta$
fw	608.79	588.04	596.66	636.93
color	yellow	yellow	yellow	yellow
cryst size (mm^3)	0.40 × 0.30 × 0.30	0.40 × 0.20 × 0.15	0.40 × 0.20 × 0.10	0.60 × 0.60 × 0.20
T, °C	−100(2)	−100(2)	−100(2)	−100(2)
λ (Mo Kα) (Å)	0.71073	0.71073	0.71073	0.71073
cryst syst	monoclinic	monoclinic	monoclinic	monoclinic
space group	$P2_1/n$	$P2_1/c$	$P2_1/c$	$P2_1/c$
a (Å)	15.4555(19)	14.683(4)	8.929(3)	9.800(5)
b (Å)	9.8213(12)	9.858(3)	18.634(5)	14.866(7)
c (Å)	18.299(2)	17.382(5)	16.412(4)	21.352(12)
α (deg)	90	90	90	90
β (deg)	91.889(2)	97.10(4)	94.86(2)	93.46(4)
γ (deg)	90	90	90	90
V ($Å^3$)	2776.2(6)	2496.7(12)	2720.9(13)	3105(3)
Z	4	4	4	4
D_{calcd} (g/cm^3)	1.618	1.564	1.457	1.362
μ(Mo Kα), cm^{-1}	56.74	45.70	41.00	37.11
F(000)	1348	1176	1208	1304
scan type	$\omega-2\theta$	$\omega-2\theta$	$\omega-2\theta$	$\omega-2\theta$
θ range, deg	1.70−28.29	2.36−22.55	2.19−22.55	1.67−22.54
no. of data [$I > 2F(I)$]	6653	3287	3583	4088
abs corr	semiempirical	semiempirical	semiempirical	semiempirical
no. of variables	212	253	271	253
R1 (wR2)[a]	0.0277 (0.0716)	0.0577 (0.1331)	0.0499 (0.0996)	0.0462 (0.1188)
goodness of fit	1.047	1.064	1.089	1.357

[a] $R1 = \sum(|F_o| - |F_c|)/\sum|F_o|$, $wR2 = (\sum[w(F_o^2 - F_c^2)^2]/\sum[(wF_o^2)^2])^{1/2}$.

The second crystal structure of **1a**/**1b** was determined on a Bruker AXS Smart 1000 X-ray diffractometer equipped with a CCD area detector and a graphite-monochromated Mo source (*K*α radiation, 0.71073 Å) and fitted with an upgraded Nicolet LT-2 low-temperature device. A suitable crystal of **1a**/**1b** was selected from their mixture in Paratone oil and mounted under a stream of N_2 at −100 °C. The ^1H NMR spectra of the crystals showed them to be a mixture of **1a** and **1b** in 0.719:0.281 molar ratio. The initial parameters, which were generated from 393 spots from all three matrix runs (20 frames each), were a = 24.34 Å, b = 9.82 Å, c = 35.35 Å, α = 90.04°, β = 100.14° and γ = 90.00°. No reasonable structure was obtained from the SHELXTL program by using this set of unit cell parameters. Preliminary unit cell and orientation matrix parameters were then obtained from a 5% sampling of the entire sphere of data. The final unit cell was developed by the program Saint (AXS-Bruker) from an analysis of the entire data set to give a = 15.4555(19) Å, b = 9.8213(12) Å, c = 18.299(2) Å, α = 90°, β = 91.889(2)°, and γ = 90°.[10] This set of parameters led to the solution of the structure of **1a**/**1b**. These observations may suggest a modulated crystal structure. The structure was solved by direct methods. Non-hydrogen atoms were anisotropically refined. Partial occupancies for Cl (0.719) and Br (0.281) were used in the refinement. All hydrogen atoms were placed in calculated positions and introduced into the refinement as fixed contributors with an isotropic U value of 0.08 $Å^2$. The calculations for the structures of **1a**/**1b** were performed with the SHELXTL (Version 5.1) software package. A search by the PLATON program finds no void spaces in this structure.[11] Since this second crystal structure of **1a**/**1b** gave smaller esd (estimated standard deviations) than the first one, it is reported in Tables 1 and 2 and Figure 1.

The crystal structures of **2**, **4**, and **5** were determined on a Siemens R3m/V diffractometer equipped with a graphite-monochromated Mo source (*K*α radiation, 0.71073 Å) and fitted with a Nicolet LT-2 low-temperature device. Suitable crystals of **2**, **4**, and **5** were coated with Paratone oil (Exxon) and mounted under a stream of N_2 at −100 °C. The unit cell parameters and orientation matrix of crystals of **2**, **4**, and **5** were determined from a least-squares fit of the orientation of at least 35 reflections obtained from a rotation photo and an automatic peak search routine. The structures were solved by direct methods. Non-hydrogen atoms were anisotropically refined. All hydrogen atoms were placed in calculated positions and introduced into the refinement as fixed contributors with an isotropic U value of 0.08 $Å^2$. The calculations for crystal structures of **2**, **4**, and **5** were performed with use of the Siemens SHELXTL 93 (Version 5.0) software package.

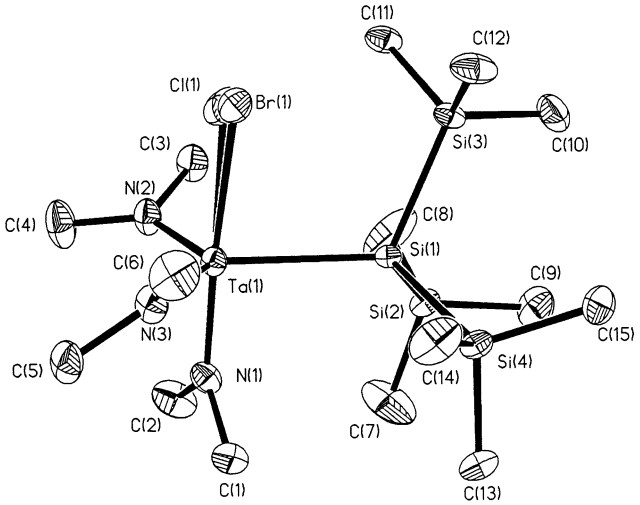

Figure 1. ORTEP of **1a**/**1b** (second crystal), showing 30% probability thermal ellipsoids. Both disordered Cl and Br atoms with partial occupancies are shown.

Results and Discussion

Synthesis and Spectroscopic Properties of 1a−5. Monosilyl complexes $(Me_2N)_3Ta(SiR_3)Cl$ [SiR_3 = $Si(SiMe_3)_3$ (**1a**), $SiPh_2Bu^t$ (**2**)] were prepared by the reactions of $(Me_2N)_3TaCl_2$[7] with $Li(THF)_3Si(SiMe_3)_3$ and $Li(THF)_3SiPh_2Bu^t$, respectively (Scheme 1). Reactions of $(Me_2N)_4TaCl$ with 1 equiv of $Li(THF)_3Si(SiMe_3)_3$ and $Li(THF)_3SiPh_2Bu^t$ yielded tetraamido silyl complexes

(10) See Supporting Information for details.
(11) Spek, A. L. *PLATON*: A Multi-Purpose Crystallographic Tool; Universiteit Utrecht: Utrecht, The Netherlands, 2002.

Scheme 1. Preparation of Ta Monosilyl Complexes 1a−4[a]

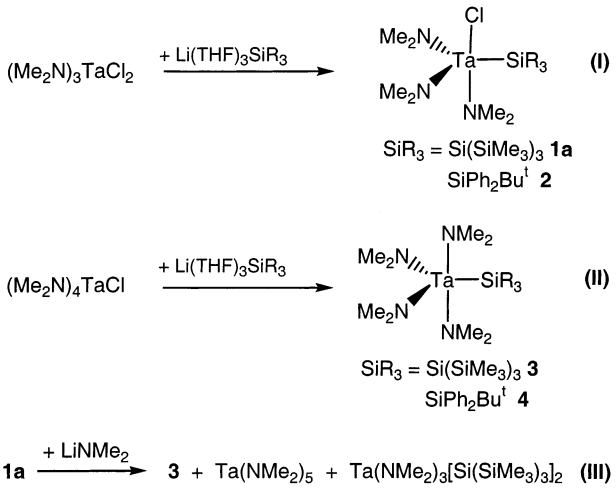

[a] Attempts to prepare **3** from the reaction of $(MeN_2)_3Ta(Cl)[Si(SiMe_3)_3]$ (**1a**) with $LiNMe_2$ only gave a mixture (III).

$(Me_2N)_4Ta(SiR_3)$ [SiR_3 = $Si(SiMe_3)_3$ (**3**), $SiPh_2Bu^t$ (**4**)] (Scheme 1). $(Me_2N)_4TaCl$ was prepared either by the metathesis reaction between $(Me_2N)_5Ta$ and $(Me_2N)_3TaCl_2$ according to a literature procedure[8] or directly from the reaction of $TaCl_5$ with $LiNMe_2$ (4:1 molar ratio) in reflux toluene. Attempts to prepare **3** by the reaction of **1** with 1 equiv of $LiNMe_2$ only resulted in the formation of a mixture of $Ta(NMe_2)_5$, **3**, and $(Me_2N)_3Ta[Si(SiMe_3)_3]_2$[6] (Scheme 1). When exposed to H_2O, **3** and **4** were found to decompose rapidly into $HNMe_2$, $HSiR_3$, and metal oxides.

$(Me_2N)_3Ta[Si(SiMe_3)_3]Cl$ (**1a**) was found to be converted to $(Me_2N)_3Ta[Si(SiMe_3)_3]Br$ (**1b**) by LiBr that was present in $Li(THF)_3Si(SiMe_3)_3$ to give a mixture of **1a** and **1b**. The addition of anhydrous LiBr and THF to a toluene-d_8 solution of such a mixture at 23 °C was found to yield **1b** (and reduce the ratio of **1a**:**1b**). This test confirmed the identification of **1b**. In our preliminary studies of a mixture of **1a** and **1b** in ca. 2:1 ratio, the two $-NMe_2$ resonances of the two complexes were assigned to an exchange in **1a**.[6] The NMR spectra of these two complexes are similar. In a ^1H EXSY spectrum (t_{mix} = 2 s) of a mixture of **1a** and **1b** at 23 °C, strong cross-peaks were observed between the $-NMe_2$ peaks of the two complexes,[10] indicating a chemical exchange process between these two complexes at this temperature. Both **1a** and **1b** are thermally unstable, and in solution slowly decompose at 23 °C.

Although **3** was clearly identified by NMR spectra, attempts to isolate a pure product were unsuccessful, as the complex slowly decomposed at room temperature to give an oily solid containing $HSi(SiMe_3)_3$ and unidentified metal-containing species. It was observed that **3** readily reacts with dry oxygen at room temperature. On exposure to dry oxygen, the orange solution of **3** gradually turned bright-yellow. The bright-yellow crystals of an oxidation product $(Me_2N)_3Ta(\eta^2\text{-}ONMe_2)[OSi(SiMe_3)_3]$ (**5**) were isolated from the reaction solution (Scheme 2). **5** was found to be inert to excess O_2. The mechanism of the reaction between **3** and O_2 is not clear, although the M−Si bond is known to be prone to oxidation by oxygen.[12] The Me_2NO moiety has been proposed as a possible intermediate in the reaction of

Scheme 2

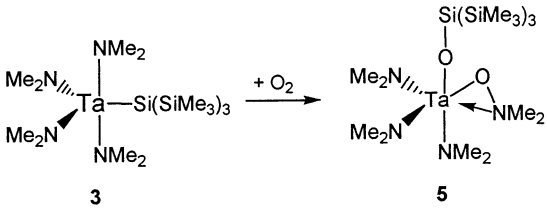

$Cr(NR_2)_3$ with O_2.[13] The direct observation of the formation of Me_2NO ligand in **5** by the oxidation of $M-NMe_2$ bond in this reaction is, to our knowledge, unprecedented.[14] The metal complexes containing R_2NO ligands usually are prepared from the corresponding hydroxyamines.[15]

The ^1H and ^{13}C NMR of **5** display two distinct resonances in 3:1 molar ratio for the $-NMe_2$ and $-ONMe_2$ ligands at 3.30 and 2.49 ppm, respectively. The NMR resonances of the $-OSi(SiMe_3)_3$ ligand in **5** are upfield shifted from those in **3**.

The ^{29}Si NMR of the α−Si atom (−51.34 ppm) of the $-Si(SiMe_3)_3$ ligand in $(Me_2N)_3Ta[Si(SiMe_3)_3]Cl/Br$ (**1a**/**1b**) is similar to that (−53.47 ppm) in $(Bu^tCH_2)_2(Bu^tCH{=})TaSi(SiMe_3)_3$.[5d] Nevertheless, the chemical shift of the α-Si atom (−98.4 ppm) in $(Me_2N)_4TaSi(SiMe_3)_3$ (**3**) is upfield-shifted from those in **1a**/**1b**. This is probably a result of the electronic effect of $-NMe_2$ ligands. There are four $-NMe_2$ ligands in **3** vs three in **1a**/**1b**. Amido ligands are known to form d−p π bonds to donate their lone-pair electrons to the electron-deficient metal centers. This likely enhances electronic shielding around the metal atoms, and thus leads to the upfield shifts of α-^{29}Si NMR resonances. A similar trend was observed in **2** and **4**. The ^{29}Si NMR of triamido silyl complex **2** (64.6 ppm) is downfield-shifted from that in $SiMe_4$ (0.00 ppm) as in some other known $-SiPh_2Bu^t$ containing complexes such as $(Me_2N)_3ZrSiPh_2Bu^t(THF)_{0.5}$ (19.6 ppm),[16a] $(Me_2N)_3HfSiPh_2Bu^t(THF)$ (46.8 ppm),[16a] $(Me_2N)_3TiSiPh_2Bu^t$ (17.8 ppm),[16a] $(Me_2N)_2[(Me_3Si)_2N]ZrSiPh_2Bu^t$ (18.1 ppm),[16a] and $(Me_3SiO)_2ZrCl(SiPh_2Bu^t)(THF)_2$ (49.6 ppm).[16b] In contrast, the ^{29}Si NMR chemical shift of the $-SiPh_2Bu^t$ ligand (−189.0 ppm) in tetraamido silyl complex **4** is significantly upfield-shifted from that in **2**. Such upfield shift has been recently observed for a sterically crowded complex $[Li(THF)_4][(Me_2N)_3Zr(SiPh_2Bu^t)_2]$ (−113.9 ppm).[6]

Solid-State Structures of 1a/1b, 2, 4, and 5. 1a and **1b** were found to co-crystallize into a crystalline mixture with disordered halide (Cl/Br) in the solid-state structure of **1a**/**1b**.[10] If the halide atom was assigned to be 100% Cl, relatively large *R* indices [R1 (*w*R2) = 0.0379

(12) Tilley, T. D. *Organometallics* **1985**, *4*, 1452.
(13) Chien, J. C. W.; Kruse, W.; Bradley, D. C.; Newing, C. W. *Chem. Commun*. **1970**, 1177.
(14) (a) Ruppa, K. B. P.; Feghali, K.; Kovacs, I.; Aparna, K.; Gambarotta, S.; Yap, G. P. A.; Bensimon, C. *J. Chem. Soc., Dalton Trans*. **1998**, 1595. (b) Odom, A. L.; Mindiola, D. J.; Cummins, C. C. *Inorg. Chem*. **1999**, *38*, 3290.
(15) Mehrotra, R. C.; Rai, A. K.; Singh, A.; Bohra, R. *Inorg. Chim. Acta* **1975**, *13*, 91.
(16) (a) Wu, Z.-Z.; Diminnie, J. B.; Xue, Z.-L. *Inorg. Chem*. **1998**, *37*, 6366. (b) Wu, Z.-Z.; Diminnie, J. B.; Xue, Z.-L. *Organometallics* **1998**, *17*, 2917. See also other related silyl complexes: (c) McAlexander, L. H.; Hung, M.; Li, L.; Diminnie, J. B.; Xue, Z.-L.; Yap, G. P. A.; Rheingold, A. L. *Organometallics* **1996**, *15*, 5231. (d) Chen, T.-N.; Wu, Z.-Z.; Li, L.-T.; Sorasaenee, K. R.; Diminnie, J. B.; Pan, H.-J.; Guzei, I. A.; Rheingold, A. L.; Xue, Z.-L. *J. Am. Chem. Soc*. **1998**, *120*, 13519. (e) Choi, S.-H.; Lin, Z.-Y.; Xue, Z.-L. *Organometallics* **1999**, *18*, 5488.

(0.1115)] were observed with the largest residual electron density 0.452 and 2.382 Å (2.683 e·Å^{-3}) away from the Cl and Ta atoms, respectively.[10] Partial occupancies with Cl and Br in the refinement (for a crystal of **1a/1b** in 0.719:0.281 molar ratio) led to a reduction in the *R* indices [R1 (wR2) = 0.0277 (0.0716)], and the largest residual electron density (1.430 e·Å^{-3}) was 4.750, 4.627, 3.972, and 1.017 Å away from the Cl, Br, Ta, and Si(4) atoms, respectively. This structure with Cl and Br partial occupancies is thus reported in Tables 1 and 2 and Figure 1.[10] In an ORTEP view of **1a/1b** (Figure 1), both the disordered Cl and Br atoms are shown. In the structure of **1a/1b**, the geometry around the Ta center can be described as a trigonal bipyramid with a silyl and two amido ligands in the equatorial and one amido and the chloride/bromide ligand on the axial positions. Such geometry is consistent with the structural assignment by NMR spectroscopy. A similar structure has been reported by Chisholm and co-workers for $(Me_2N)_3Ta(p\text{-tolyl})Br$[8] in which one NMe_2 and the bromide ligands occupy the axial positions.

The trans angles of N(1)−Ta−Cl [178.1(2)°] and N(1)−Ta−Br [174.6(2)°] in **1a/1b** and are close to that [173.1(2)°] in $(Me_2N)_3Ta(p\text{-tolyl})Br$.[8] All equatorial ligands are slightly bent toward the chloride/bromide. The angles of the chloride and bromide in **1a/1b** to Si(1), N(2), and N(3) range from 87.3(2) to 89.7(2)° and 84.16(19) to 93.5(2)°. The angles of N(1) on the axial NMe_2 ligand to Si(1), N(2), and N(3), in comparison, range from 90.06(11) to 92.95(8)°.

The Ta−Si bond distance of 2.7167(8) Å in **1a/1b** is comparable to those in $Cp^*_2(ArN{=})Ta_2H_2(\mu\text{-}ArNSiHPh)$ [2.709(1) Å; Ar = 2,6-$Pr^i_2C_6H_3$][4g] and $[(Me_3Si)_2N](Me_2N)(Me_3SiN{=})Ta(SiPh_2Bu^t)$ [2.704(2) Å],[4i] and is slightly longer than those in $Cp^*_2Ta_2H_2(\mu\text{-}ArNSiHPh)_2$ [2.695(3) Å],[4g] $(RCH_2)_2(RCH{=})TaSi(SiMe_3)_3$ [R = Bu^t, 2.680(15) Å;[4d] $SiMe_3$, 2.611(7) Å[4e]], $(C_5Me_5)Ta(SiMe_3)Cl$ [2.669(4) Å],[4b] $(Me_3SiCH_2)_2Ta(\mu\text{-}CSiMe_3)_2Ta(CH_2SiMe_3)[Si(SiMe_3)_3]$ [2.666(3) Å],[4f] $Cp_2Ta(H)_2SiPh_2Me$ [2.651(4) Å],[4a] $Cp_2Ta(H)(SiMe_2H)_2$ [2.624(2)−2.633(2) Å],[4c] and $CpTa(SiMe_2Cl)(H)(PMe_3)[{=}N(2,6\text{-}Pr^iC_6H_3)]$ [2.574(1) Å].[4h] The Ta−N bond distances in **1a/1b** range from 1.927(3) to 1.984(4) Å, and are comparable to those in, e.g., $[(Me_3Si)_2N](Me_2N)(Me_3SiN{=})Ta(SiPh_2Bu^t)$.[4i]

In the crystalline state, **2** is composed of discrete $(Me_2N)_3Ta(SiPh_2Bu^t)Cl$ molecules. An ORTEP view of the molecule giving the atom numbering scheme is shown in Figure 2. Bond distances and angles are given in Table 3. The molecule adopts a distorted trigonal bipyramidal geometry in the solid state. The structure of **2** is similar to that of **1a/1b** with the silyl ligand in the equatorial and chloride in the axial positions. The trans angle of 174.5(4)° and the Ta−Si bond distance of 2.726(4) Å in **2** are close to those in **1a/1b**. The Ta−N bond (axial) [1.989(11) Å] is longer than the equatorial Ta−N bonds [1.946(11) and 1.926(11) Å]. The Ta−Cl bond distance of 2.454(3) Å is comparable to the terminal Ta−Cl bond distances in $(Me_2N)_2(Me_2NH)TaCl_3$ [2.391(2)−2.450(2) Å],[7] $[(Me_2N)_2(Me_2NH)TaCl_2]_2O$ [2.417(2) and 2.505(2) Å],[7] $[(Me_2N)_3TaCl_2]_2$ [2.463(1) Å],[7] and $[(Me_3Si)N]_2TaCl_3$ [2.351(2)−2.362(2) Å].[17]

An ORTEP view of **4** is shown in Figure 3. Selected bond distances and angles are listed in Table 4. The structure of **4** is similar to those of **1a/1b** and **2** and adopts a trigonal bipyramidal geometry with the silyl ligands in the equatorial positions. However, a related alkyl amido complex $(Me_2N)_4TaBu^t$ adopts a square-pyramidal structure with *tert*-butyl ligand in the axial position.[8] Compared to **1a/1b** and **2**, the trans angle [170.4(4)°] in **4** is smaller. Interestingly, both axial $-NMe_2$ ligands are slightly bent toward the $-SiPh_2Bu^t$ ligand. This suggests that the steric repulsion between amido ligands is perhaps greater than that between amido and silyl ligands as the Ta−Si bond is longer than Ta−N bonds.

The Ta−Si bond distance of 2.754(3) Å in **4** is longer than those in **1a/1b**, **2**, and other known Ta(V) silyl complexes. To our knowledge, it is the longest Ta−Si bond among reported Ta(V) silyl complexes. The long Ta−Si bond in **4** is probably a result of the steric effect, although the electronic influence of the NMe_2 ligand

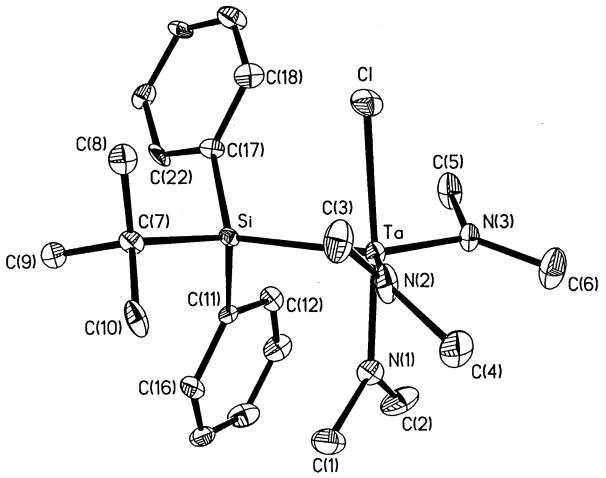

Figure 2. ORTEP of **2**, showing 35% probability thermal ellipsoids.

Table 2. Selected Bond Distances (Å) and Angles (deg) in 1a/1b

Ta(1)−Si(1)	2.7167(8)	Ta(1)−Cl(1)	2.512(7)
Ta(1)−Br(1)	2.575(6)	Ta(1)−N(1)	1.984(3)
Si(1)−Si(2)	2.3609(10)	Ta(1)−N(2)	1.927(3)
Si(1)−Si(3)	2.3725(10)	Ta(1)−N(3)	1.967(3)
Si(1)−Si(4)	2.3689(11)		
Cl(1)−Ta(1)−N(1)	178.1(2)	Br(1)−Ta(1)−N(1)	174.6(2)
Cl(1)−Ta(1)−N(2)	89.7(2)	Br(1)−Ta(1)−N(2)	93.5(2)
Cl(1)−Ta(1)−N(3)	88.2(2)	Br(1)−Ta(1)−N(3)	87.6(2)
Cl(1)−Ta(1)−Si(1)	87.3(2)	Br(1)−Ta(1)−Si(1)	84.16(19)
Cl(1)−Ta(1)−Br(1)	4.2(4)	N(1)−Ta(1)−N(2)	91.84(11)
Si(1)−Ta(1)−N(1)	92.95(8)	N(1)−Ta(1)−N(3)	90.06(11)
Si(1)−Ta(1)−N(2)	118.41(10)	N(2)−Ta(1)−N(3)	119.00(14)
Ta(1)−Si(1)−Si(2)	114.77(3)	Ta(1)−Si(1)−Si(3)	114.06(3)
Ta(1)−Si(1)−Si(4)	113.72(4)	Si(2)−Si(1)−Si(3)	103.75(4)
Si(2)−Si(1)−Si(4)	104.57(4)	Si(3)−Si(1)−Si(4)	104.81(4)

Table 3. Selected Bond Distances (Å) and Angles (deg) in 2

Ta−Si	2.726(4)	Ta−Cl	2.454(4)
Ta−N(1)	1.989(11)	Si−C(7)	1.937(13)
Ta−N(2)	1.946(11)	Si−C(11)	1.887(12)
Ta−N(3)	1.926(11)	Si−C(17)	1.917(13)
Cl−Ta−N(1)	174.5(4)	Si−Ta−N(1)	87.4(3)
Cl−Ta−N(2)	88.6(4)	Si−Ta−N(2)	120.9(3)
Cl−Ta−N(3)	93.9(3)	Si−Ta−N(3)	118.6(4)
Cl−Ta−Si	88.10(12)	N(1)−Ta−N(2)	91.0(5)
N(1)−Ta−N(3)	91.1(5)	N(2)−Ta−N(3)	120.5(5)

(17) Bradley, D. C.; Hursthouse, M. B.; Abdul Malik, K. M.; Vuru, G. B. C. *Inorg. Chim. Acta* **1980**, *44*, L5.

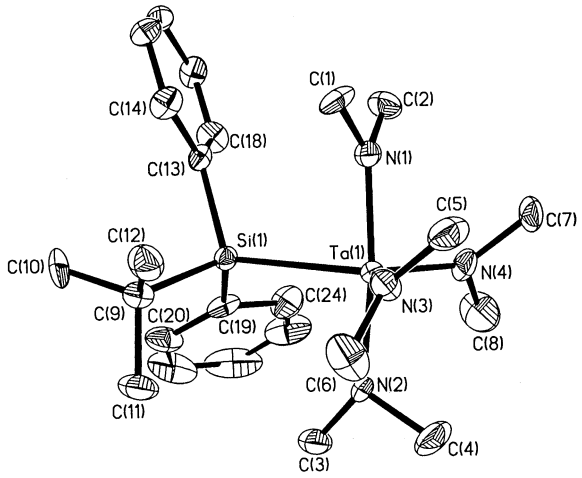

Figure 3. ORTEP of **4**, showing 35% probability thermal ellipsoids.

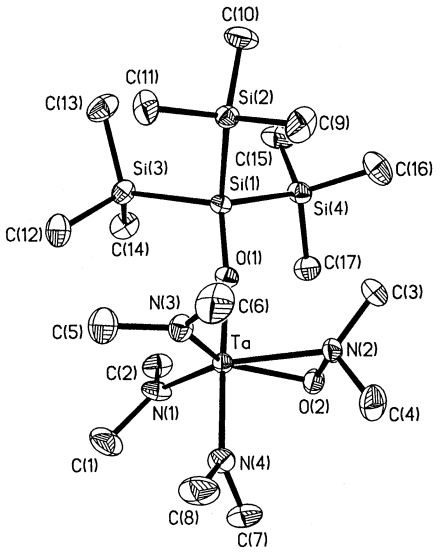

Figure 4. ORTEP of **5**, showing 35% probability thermal ellipsoids.

Table 4. Selected Bond Distances (Å) and Angles (deg) in 4

Ta(1)−Si(1)	2.754(3)	Ta(1)−N(4)	1.979(11)
Ta(1)−N(1)	2.009(9)	Si(1)−C(9)	1.955(13)
Ta(1)−N(2)	2.029(10)	Si(1)−C(13)	1.929(12)
Ta(1)−N(3)	1.979(10)	Si(1)−C(19)	1.893(12)
N(1)−Ta(1)−N(2)	170.4(4)	Si(1)−Ta(1)−N(1)	84.3(3)
N(1)−Ta(1)−N(3)	92.7(4)	Si(1)−Ta(1)−N(2)	86.8(3)
N(1)−Ta(1)−N(4)	90.2(4)	Si(1)−Ta(1)−N(3)	117.8(3)
N(2)−Ta(1)−N(3)	94.8(5)	Si(1)−Ta(1)−N(4)	123.4(3)
N(2)−Ta(1)−N(4)	91.5(5)	N(3)−Ta(1)−N(4)	118.8(5)

cannot be ruled out. Steric effect perhaps also made the Ta−N bond distances [1.979(11)−2.029(10) Å] longer than those in **1a**/**1b** and **2**.

An ORTEP view of **5** is shown in Figure 4. Selected bond distances and angles are listed in Table 5. The geometry around the Ta center can be best described as a pseudo-trigonal bipyramid with the η^2-ON unit occupying a single coordination site. The trans angle of O(1)−Ta−N(4) [176.0(4)°] is close to those found in **1a**/**1b**, **2**, and **4**. The angles within the Ta(η^2-ON) unit are unexceptional and close to those in other dialkylhydroxylamino complexes such as $MoO_2(ONEt_2)_2$,[18] $V_2O_2(ONEt_2)_4$,[18] and $Ti(ONEt_2)_4$.[19] The O−N bond distance of 1.466(13) Å is close to those in $MoO_2(ONEt_2)_2$ [1.427(3) Å],[18] $V_2O_2(ONEt_2)_4$ [1.402(2) Å],[18] and $Ti(ONEt_2)_4$ [1.402(7) Å].[19] The Ta−N(2) bond [2.254(9) Å] is significantly longer than other Ta−NMe_2 bonds in **5** [1.999(10)−2.037(10) Å]. This is perhaps indicative of the dative bonding nature of the Ta−N(2) bond in **5** (Scheme 2). Two Ta−O bonds [1.991(8) Å] are close to those in $Ta(CH_2SiMe_3)(O_2CNMe_2)_4$[8] and $[(Me_2N)_2(Me_2NH)TaCl_2]_2O$.[7]

Table 5. Selected Bond Distances (Å) and Angles (deg) in 5

Ta−O(1)	1.991(8)	Si(1)−O(1)	1.633(8)
Ta−O(2)	1.991(8)	Si(1)−Si(2)	2.353(5)
Ta−N(1)	2.006(10)	Si(1)−Si(3)	2.363(5)
Ta−N(2)	2.254(9)	Si(1)−Si(4)	2.360(5)
Ta−N(3)	1.999(10)	N(2)−O(2)	1.466(13)
Ta−N(4)	2.037(10)		
O(1)−Ta−N(1)	89.4(3)	N(1)−Ta−N(2)	151.0(4)
O(1)−Ta−N(2)	89.4(3)	N(1)−Ta−N(3)	113.3(4)
O(1)−Ta−N(3)	95.9(4)	N(1)−Ta−N(4)	88.9(4)
O(1)−Ta−N(4)	176.0(4)	N(2)−Ta−N(3)	95.6(4)
O(1)−Ta−O(2)	88.9(3)	N(2)−Ta−N(4)	90.2(4)
O(2)−Ta−N(1)	111.2(4)	N(3)−Ta−N(4)	88.1(4)
O(2)−Ta−N(3)	135.2(4)	O(2)−Ta−N(4)	88.3(4)
Si(1)−O(1)−Ta	169.1(5)	N(2)−O(2)−Ta	79.8(5)
O(2)−N(2)−Ta	60.4(4)		

We have reported synthesis and characterization of Ta(V) alkyl alkylidene silyl complexes $(RCH_2)_2Ta(=CHR)SiR'_3$ [R = CMe_3, $SiMe_3$; $R'_3 = (SiMe_3)_3$, Ph_2Bu^t].[4d,e] Attempts to prepare tetra(alkyl) silyl Ta(V) complexes by using β-hydogen free alkyl ligands have been unsuccessful; α-hydrogen abstraction by the silyl reagents was observed. Using strong π-donor ligand NMe_2, we were able in the current work to prepare a series of Ta(V) silyl complexes with σ-bonded ligands through direct substitution reactions.

Acknowledgment is made to the National Science Foundation (CHE-9904338 and CHE-0212137), Camille Dreyfus Teacher−Scholar award, Ziegler Research Fund, and DuPont Young Professor program for financial support of this research. We thank the referees for helpful suggestions, Dr. Donald H. Berry for the interpretation of the NMR of **1a** and **1b**, and Drs. Craig E. Barnes, Carolyn B. Knobler, and Saeed Kahn for assistance with the X-ray structure of **1a**/**1b**.

Supporting Information Available: A complete list of the crystallographic data for **1a**/**1b** (the first and second crystal structures; in the latter, both the data for Cl and Br in partial occupancies and for 100% Cl), **2**, **4**, and **5**, an ORTEP view of the first crystal of **1a**, and the EXSY spectrum of a mixture of **1a**/**1b** and $(Me_2N)_3Ta[Si(SiMe_3)_3]Br$ (−NMe_2 region). This material is available free of charge via the Internet at http://pubs.acs.org.

OM020537G

(18) Saussine, L.; Mimoun, H.; Mitschler, A.; Fisher, J. *Nouv. J. Chim.* **1980**, *4*, 235.
(19) Wieghardt, V. K.; Tolksdorf, I.; Weiss, J.; Swirdoff, W. *Z. Anorg. Allg. Chem.* **1982**, *490*, 182.